

The Effects of Curing Temperature on the Hydration Kinetics of Plain and Fly Ash Pastes and Compressive Strength of Corresponding Mortars with and without nano-TiO₂ Addition

D. Huang, M. Velay-Lizancos, and J. Olek

Lyles School of Civil Engineering, Purdue University

ABSTRACT

Incorporation of fly ash in cementitious systems containing ordinary portland cement (OPC) increases their long-term strength and durability. However, replacement of cement by fly ash also reduces the heat of hydration of such systems and reduces early-age strength development. The reduced rate of strength development can increase the risk of durability problems, e.g. scaling, in cases when young concrete is exposed to low temperatures and deicing chemicals. This study investigated the potential of nano-titanium dioxide (nano-TiO₂) particles to modify the hydration kinetics of fly ash pastes and compressive strength development of corresponding mortars cured under low (4°C) and standard (23°C) temperatures. The kinetics of the hydration study was performed on paste specimens using the thermogravimetric analysis (TGA) and isothermal calorimetry (IC) methods. The mortar specimens used for compressive strength testing were prepared using the same w/cm values and the same types of binders as those used to prepare the paste specimens. It was found that although the addition of nano-TiO₂ accelerated the hydration rate of all pastes, that treatment was, however, more effective in the fly ash pastes than in the ordinary portland cement (OPC) pastes, especially for the cases of low temperature curing. These findings were confirmed by the results of strength testing as the specimens experiencing accelerated rates of hydration were also found to be stronger.

Keywords: Fly ash, TiO₂ nanoparticles, TGA, Hydration, Isothermal calorimetry, Strength

1. INTRODUCTION

The supplementary cementitious materials (SCMs) may affect the hydration process of the cement phases by two principal mechanisms: a) at the same overall w/cm value, the effective water-to-cement ratio will be higher when part of the cement is replaced by SCMs. Therefore, more space is available for the hydration products of the cement phases; b) SCMs provide extra surfaces as nucleation sites, thus promoting a higher degree of hydration [1]. In addition to modifying the kinetic of cement hydration, the use SCMs generally benefits both fresh and hardened properties of concrete, including: improvements of pumpability and finishability, decrease in permeability, mitigation of alkali reactivity, and overall improvement of hardened properties of concrete through either hydraulic or pozzolanic activity, or both [2][3][4][5][6]. As a result, the use of SCMs typically results in more durable concrete in the long term [7][8][9].

However, replacing cement with some of the SCMs, such as fly ash and slag cement, will generally result in slower early strength development (especially at high-levels of replacement) [10]. In particular, scaling

resistance of concrete with fly ash and slag SCMs can be negatively affected, especially when such

concretes are exposed to deicing chemicals before reaching full maturity [11]. Researchers also pointed out that the peak of the heat of hydration of OPC-fly ash samples is essentially delayed compared to the OPC-only samples at an early age [10][12].

The available literature reports that some the bulk characteristics (e.g., mechanical properties, durability) of the cement-based composites can be modified by various types of nanoparticles [13][14]. Nano-titanium dioxide (nano-TiO₂) is one of the nanomaterials materials that have been investigated extensively in concrete applications [15][16][17]. However, very little information is available on the effects of nano-TiO₂ on the cementitious composites containing fly ash when exposed to low curing temperatures.

This study compares the influence of various levels of nano-TiO₂ addition on kinetics of hydration and the strength development of, respectively, plain and fly ash cement pastes and mortars exposed to both standard (room) temperature (23°C) and low (4°C)

temperature. The thermogravimetric analysis (TGA) and the isothermal calorimetry (IC) methods were used to study how the different levels of nano-TiO₂ influence the hydration process of the pastes. In addition, the thermal indicators of the setting time for each cement paste were estimated from IC data. Furthermore, mortar specimens were prepared to study the influence of nano-TiO₂ on the compressive strength development.

2. MATERIALS AND METHODS

2.1. Materials and sample preparation

The OPC and fly ash paste samples with the various levels of nano-TiO₂ addition were made in the laboratory for use in this study. Nano-TiO₂ particles (with an average particle size of 18 nm) were purchased from US Research Nanomaterials, Inc. Figure 1 shows the image of the cluster of the particles of the nano-TiO₂ provided by the company. The XRD analysis of the nano-TiO₂ particles has shown that the only phase present in the material was anatase (see Figure 2). Physical properties of the nano-TiO₂ particles used are provided in Table 1.

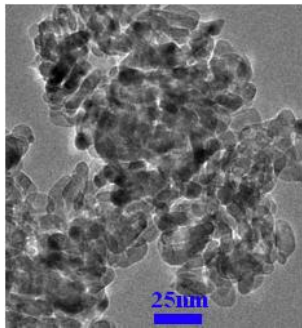


Figure 1. Transmission electron microscope image of the particles of nano-TiO₂ (courtesy of the US Research Nanomaterials, Inc.).

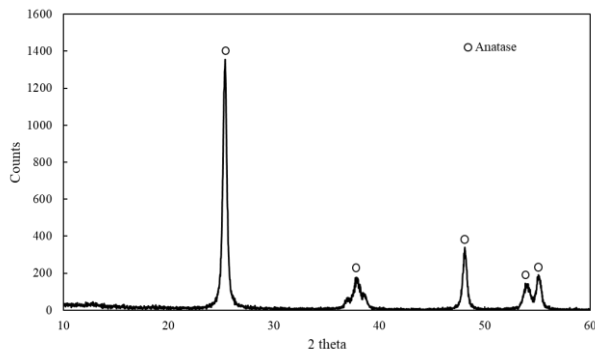


Figure 2. XRD patterns of nano-TiO₂ used in the study.

Table 1. Physical properties of TiO₂ nanoparticles.

Purity	APS*	SSA*	Density
99.9%	18nm	200-240 m ² /g	0.24 g/cm ³

*APS: average particle size;

*SSA: specific surface area.

The ASTM C150M-21 [18] Type I Portland cement (OPC) used in this study was produced by Buzzi Unicem USA, and its chemical composition is provided in Table 2.

Table 2. Composition of the Portland cement (wt. %)

Item	SiO ₂	Al ₂ O ₃	Fe ₂ O ₃	CaO	MgO	SO ₃	LOI
Content	19.55	5.22	2.74	62.91	2.94	3.22	2.25

The ASTM C618-19 [19] Class C fly ash (FA) was purchased from Boral Resources. The ASTM C494-19 [20] high-range water-reducing admixture (HRWR) was supplied by the BASF and used during mixing to ensure adequate level of workability and aid with the dispersion of nano-TiO₂ [15]. A constant amount of HRWR (0.25 wt. % of the total weight of the cementitious materials) was used in all mixtures. Different levels (0%, 0.5%, 1%, and 2%) of nano-TiO₂ were added as the weight percentages (wt. %) of the total cementitious materials (i.e., the total weight of OPC or OPC+FA). The mixture proportions of pastes used in this study are shown in Table 3. Mortars specimens were prepared using the same mixture designs but with adding natural siliceous sand satisfying Indiana Department of Transportation (INDOT) standard Specification 900 for No. 23 fine aggregate [21]. The weight ratio of sand to cementitious material was 2.48:1.

Table 3. Mixture proportions of cement pastes used in the study. (Ratios are calculated on weight basis)

Sample type	Sample	FA/O PC	Water/(FA+ OPC)	Nano-TiO ₂ (wt.%)
Paste	OPC-0T	\	0.45	0
	OPC-0.5T	\	0.45	0.5
	OPC-1T	\	0.45	1.0
	OPC-2T	\	0.45	2.0
	FA-0T	0.313	0.45	0
	FA-0.5T	0.313	0.45	0.5
	FA-1T	0.313	0.45	1.0
	FA-2T	0.313	0.45	2.0

All component materials were conditioned at room temperature and weighted before mixing. Paste and mortar samples were prepared according to the requirements of ASTM C305-20 [22]. Water and HRWR were pre-mixed in a small container first, and then the nano-TiO₂ was added into the same container. The resulting liquid was then transferred to the mixing bowl of the mechanical mixer. For mortars specimens, the fine aggregate was added in the following step. Finally, OPC and FA were added and all materials were mechanically mixed. Once mixed, the fresh mortars were used to cast 50 × 50 × 50 mm cubes (for compressive strength testing). The specimens were stored in the molds for 24 hours (at 23 °C and 50% RH). After that, mortar specimens

were demolded and cured at two different temperatures (room (or standard) = 23°C and low = 4°C) until the time of testing (3, 7, and 28 days). The compressive strength testing was performed according to the ASTM C109M-21 [23]. Paste specimens used in the TGA test were prepared using the same mixing process as that used for mortars, except that the sand was excluded from the list of the ingredients. The TGA pastes were cast in cylindrical plastic containers, diameter of 25 mm and the height of 12 mm, and cured in the same way as mortar specimens. To prepare pastes for IC test, the mixing water and the cementitious materials, as well as the glass mixing rod and the glass mixing vessel, were all conditioned at the corresponding temperatures (23°C or 4°C) for at least 24 h before mixing. At the end of the conditioning period, the water was added to the cementitious material contained in the glass vessel and mixed using the glass rod. The resulting paste was then is transferred to the ampules used for the IC test.

2.2. Research Methodology

2.2.1. Determination of the quantities of hydration products

To conduct the TGA test, paste specimens were removed from the curing room at the desired testing ages (3, 7, and 28 days) and small pieces of the material were broken-off from the body of the cylinder. These broken-off pieces were then immersed for 10-15 min. in isopropanol in order to replace the pore water and thus stop the hydration process [24]. Subsequently, the isopropanol was washed-off from the samples by soaking them in the diethyl ether for 30 sec. Samples were then dried in an aerated oven for no more than 10 min. and ground to pass the #200 (75µm) sieve. The weight percentage of hydration products was determined using the TA Instruments 2050 thermogravimetric analyzer. During the test, the powder samples were heated up from room temperature (around 20°C) to 900°C at a constant rate of 10 °C/m. The sizes of samples were around 20 mg. A 99.9% pure N₂ gas was used as a purge gas to provide an inert environment when operating the TGA instrument.

Table 4 shows the physical and chemical processes (and the corresponding temperature ranges) taking place in a typical cementitious systems during the TGA testing [25]. As it can be seen, these processes are mainly associated with decomposition of C-S-H, ettringite, and calcium hydroxide (CH) phases, which are the most abundant hydration products in cementitious systems based on the OPC [26]. In general, most of the hydration products lose water from the beginning of the TGA test (about 20°C) up to

the end of decomposition of CH phase (around 450°C).

2.2.2. Determination of the rate of hydration of pastes

In this study, the isothermal calorimeter (IC) test was used to study the kinetics of hydration of cementitious materials with and without the addition of nano-TiO₂ and cured at different temperatures. The total heat evolved, and the rate of heat production (thermal power) were measured by IC (Tam Air, TA instruments) following ASTM C1702-17 [27] at both room temperature (23°C) and low temperature (4°C).

Table 4. Physical and chemical changes in concrete as a function of temperature (adopted for ref. [25]).

Temperature (°C)	Physical/chemical effect
20-200	Loss of capillary water
70-80	Dissociation of ettringite
120-160	Dehydration of gypsum to hemihydrate and anhydrite
200-350	Loss of bound water from cement paste (C-S-H)
400-450	Calcium hydroxide (CH) loses water
575	Quartz changes from α to β form (volume increase)
600-850	Decomposition of carbonates

After mixing (detailed procedure was previously described in Section 2.1), around 10 grams of paste was transferred to the glass ampules which were placed inside the calorimeter. The entire process (from combining the cementitious materials with water to placing the ampules in the calorimeter) took less than 5 min. The data collected during the initial 45 min. after mixing of water with cementitious materials were excluded from the analysis as the samples were in the process of thermal equilibration. The measurements were performed over a period of up to 50 h from the time of the addition of water.

2.2.3 Determination of thermal indicator of the setting time

According to ASTM C1679-17 [28], the IC test results can be used to determine so called “thermal indicator of setting time” of cementitious mixtures, which is defined as “the hydration time to reach a thermal power of 50% of the maximum value of the main hydration peak”. This data was used as a supplementary information to aid in evaluating the effects of nano-TiO₂ on the hydration process of cement pastes characterized in this study.

2.2.4 Compressive strength of mortars

The compressive strength of mortar specimens, with and without the fly ash and nano-TiO₂, cured at both, the room and low temperatures, were measured at the ages of 3, 7, and 28 days. The compressive

strength was determined using the MTS testing machine following the provisions of ASTM C109M-21 [24] standard specification.

3. RESULTS AND DISCUSSION

3.1 Hydration kinetics of nano-TiO₂ modified pastes

In principle, the changes in the content of calcium hydroxide (CH) in the hydrating cementitious system can be used to evaluate the kinetic of hydration as CH is a byproduct of the primary hydration reaction. This approach works well in cases when the only cementitious binder present in the hydrating system is the ordinary Portland cement (OPC). However, the CH content might not be a good indicator of the kinetic of hydration in samples with the blended binders (e.g., in the system containing both, the cement and the fly ash, as was the case in the current study). This is because the changes in the CH content will reflect the combined effects of cement hydration (addition of CH) and pozzolanic reaction (consumption of CH). Therefore, instead of focusing exclusively on the changes in the CH content (associated with the weight loss in the temperature range from 400°C to 450°C in TGA test) as an indicator of the hydration process, a broader temperature range should be considered when evaluating the amount of hydration products when fly ash is present as part of the cementitious binder.

In this study, the temperature range selected for evaluation of the influence of nano-TiO₂ on the hydration process of OPC and fly ash pastes was from 20°C to about 450°C (the temperature where the CH decomposition ends). Since, as mentioned in section 2.2.1, the free water initially present in the specimens was removed by the solvent exchange procedure, any weight changes taking place in this broader temperature range should only capture the removal of the chemically/structurally bound water in the phases of interest, i.e. C-S-H, ettringite, monosulfate, CH, and other hydration products. As mentioned earlier (section 2.2.1 and Table 4), changes in the amounts of these phases can be used as indicators of the kinetics of hydration as higher weight losses will indicate higher amount of hydration products, and thus an accelerated rate of the hydration process.

3.1.1 The influence of nano-TiO₂ on the amount of the hydration products.

As an example of the TGA results, Figure 3 shows the TGA curves for OPC pastes with and without nano-TiO₂ cured for 3 days at low temperature. The solid green line represents the TGA results from the reference sample OPC-0T (0 wt.% of nano-TiO₂ addition), whereas the dashed green line represents paste containing 2% of nano-TiO₂ (OPC-2T). It can be

seen that the amount of hydration products (assumed to be equivalent to the weight loss in the temperature range from 20°C to about 450°C) increases due to the addition of nano-TiO₂. This means that for this particular case (3 days of curing at low temperature), the addition of nano-TiO₂ accelerates the hydration process. Such acceleration of hydration can be explained by the fact that nano-TiO₂ particles serve as the nucleation sites for the formation of the C-S-H.

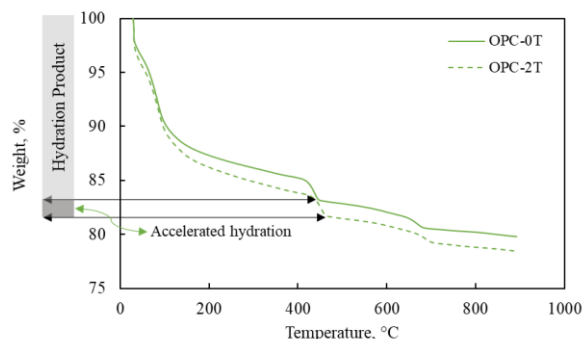


Figure 3. The TGA results for OPC paste with 0% and 2% of TiO₂ nanoparticles cured for 3 days at low temperature.

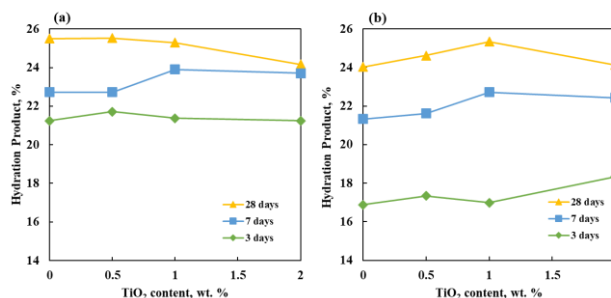


Figure 4. The amounts of hydration products in the OPC pastes with different levels of nano-TiO₂ addition after 3, 7, and 28 days of curing at: (a) room temperature and, (b) low temperature.

The overall trends in the amounts of the hydration product obtained from TGA results for the OPC pastes with varying amounts of added nano-TiO₂ and cured for 3, 7, and 28 days at room and low temperatures are presented in Figures 4(a) and (b), respectively. For pastes cured at room temperature, the addition of nano-TiO₂ accelerated the hydration process at early ages (3 and 7 days, green and blue lines, respectively), but not at later age (28 days-yellow line). It can also be seen that the lines representing 3 days and 7 days results essentially plateaued past the 1.0 wt.% of nano-TiO₂ addition. Similar observations are reported by other researchers [29]–[31]. Many argue that a higher dosage of nano-TiO₂ can limit the space available for the growth of various hydration products within the cementitious system. This hypothesis is, to certain extent, corroborated by the results from specimens cured for 28 days, which show the decreasing trend in the amount of hydration products with the increase in the addition level of the

nano-TiO₂ past 0.5% (solid yellow line). In this case, it is likely that most of the hydrating phases have already reacted at the end of 28-days and that the addition of higher amounts of nano-TiO₂ is not promoting more hydration due to the lack of space.

When the same type of samples was cured at low temperature, see Figure 4(b), the addition of nano-TiO₂ also seems to have accelerated the hydration process. When compared to specimens cured at room temperature, the acceleration happened at both, later ages and at higher contents of nano-TiO₂. As evident from the trends shown by the green and blue lines in Figure 4(b), 2.0 wt.% addition of nano-TiO₂ can still accelerate the hydration process of OPC pastes cured at low temperature at 3 days and the addition of up to 1% of nano-TiO₂ accelerates the hydration process for both, 7 days and 28 days hydration periods. It seems, therefore, that since the low temperature significantly slows down the hydration process, the addition of nano-TiO₂ is more effective when compared to its effects at room temperature.

In conclusion, data presented in Figure 4 indicate that the addition of nano-TiO₂ is more effective in accelerating the hydration process of OPC pastes cured at low temperature compared to those cured at room temperature.

Figures 5(a) and 5(b) present the amounts of hydration product obtained from the TGA results for fly ash pastes with different levels of nano-TiO₂ addition after 3, 7, and 28 days of curing at: (a) room temperature and (b) low temperature. The trends shown in Figure 5(a) are similar to those shown in Figure 4(a), i.e. the addition of nano-TiO₂ accelerates the hydration process at early ages (3 and 7 days) when cured at room temperature. However, as indicated by the slopes of the green and blue lines, a more significant acceleration of hydration was observed in fly ash pastes as compared to plain (OPC only) pastes, especially at early ages. This might be because, besides providing nucleation sites for the formation of the C-S-H, the addition of nano-TiO₂ was also reported to reduce the size of CH crystals [15]. The smaller crystals may be accelerating the rate of the pozzolanic reaction, thus producing higher amount of C-S-H (and other hydrates) which will lead to higher weight losses in the fly ash pastes in the temperature range of interest (20°C to about 450°C).

As shown in Figure 5(b), the addition of nano-TiO₂ also accelerates the hydration process of fly ash pastes cured at low temperature. When comparing the 7 days and 28 days data for 1% addition of nano-TiO₂ (shown in Figure 5(b)), it can be seen that the amounts of hydration products formed at these two ages were very comparable. Such effect was not

observed in OPC pastes cured at low temperature (Figure 4(b)). This observation further confirms that in systems cured at low temperature, the nano-TiO₂ is more effective in fly ash pastes than in OPC pastes.

From the comparison of Figures 4 and 5, it seems that a higher content of nano-TiO₂ is more beneficial at earlier ages (3 and 7 days), irrespective of binder composition and curing temperature. These findings are in agreement with those reported by other researchers [32].

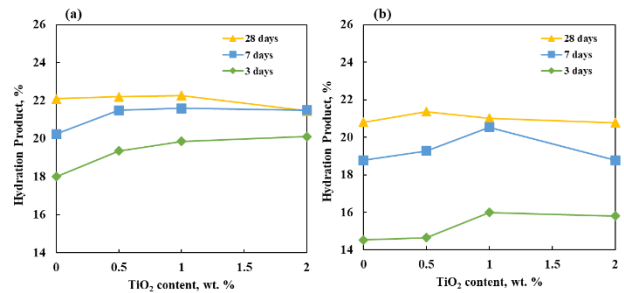


Figure 5. The amounts of hydration products in the fly ash pastes with different levels of nano-TiO₂ addition after 3, 7, and 28 days of curing at: (a) room temperature and (b) low temperature.

3.1.2 Influence of nano-TiO₂ on the QI_{ahp} in fly ash pastes

In order to appraise the relative increase in the amount of hydration products formed in fly ash pastes (with respect to the reference sample, i.e. the sample without the addition of nano-TiO₂), we introduce the parameter QI_{ahp} (a quantitative increase in the amount of hydration product). The value of the QI_{ahp} was calculated using Eq. 1 (below).

$$QI_{ahp} = \frac{W_x - W_0}{W_0} \quad \text{Eq. (1)}$$

Where: W_x = weight loss in specimens with “x” % nano-TiO₂ and W_0 = weight loss in specimens with 0 % nano-TiO₂.

The values of the QI_{ahp} for pastes cured for 3, 7, and 28 days at both, the standard (room) and low temperatures, are shown in, respectively, Figures 11(a) and 11(b). As can be seen, the values of QI_{ahp} for different ages follow the sequence: 3 days > 7 days > 28 days. That sequence confirms the previously discussed trends (see section 3.1.1), indicating that nano-TiO₂ is more effective in accelerating the hydration process at earlier ages, regardless of the curing temperature.

As shown in Figure 6(a), the amount of hydration product increases with the increase in the amount of nano-TiO₂ addition (up to 2.0 wt.%) at early ages (3 and 7 days). However, the addition of 2.0 wt.% of nano-TiO₂ negatively affects the amount of hydration

products at 28 days. Several previously published works also reported on diminishing effectiveness of increased dosages of nano-TiO₂ with respect to improving the properties of cementitious materials [29][30][31]. Some of the reasons for this behavior might be related the difficulty in achieving a good dispersion of higher amounts of nano-TiO₂ within the cementitious system. More importantly, some researchers, e.g. [29], argue that higher content of nanoparticles can effectively reduce the distance between the particles in the cementitious system and thus limit the space available for growth of the hydration products. Moreover, as already mentioned in section 3.1.1, for specimens which are cured at room temperature, by the age of 28 days most of the hydrating phases have likely already reacted, thus limiting the effectiveness of nano-TiO₂ addition.

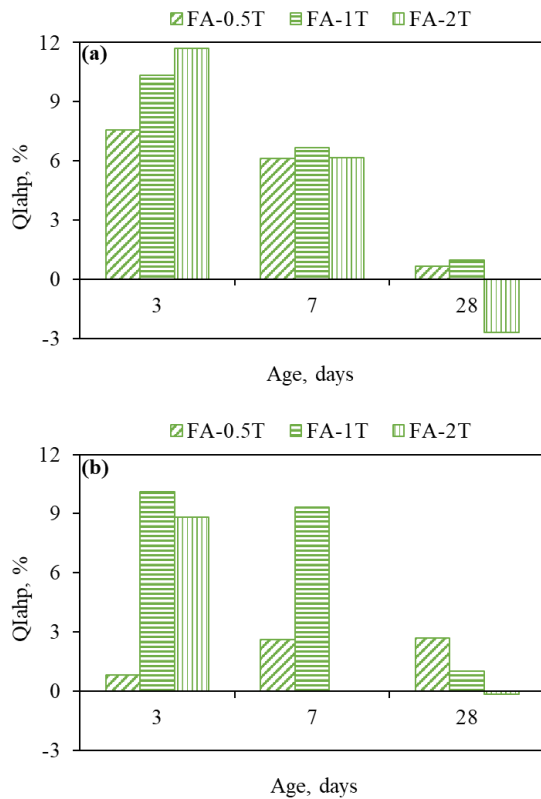


Figure 6. The values of Q_{ahp} (quantitative increase in the amount of hydration products) for fly ash pastes cured for 3, 7, and 28 days cured at: (a) room temperature and, (b) low temperature.

For fly ash pastes cured at low temperature (Figure 6(b)), the addition of nano-TiO₂ seems to be more beneficial in accelerating the hydration at 28 days compared to pastes cured at room temperature (Figure 6(a)).

3.2 Rate of hydration of nano-TiO₂ modified pastes

To study the influence of curing temperatures on the effect of nano-TiO₂ on the rate of hydration of OPC and fly ash pastes, 8 different types of mixtures were prepared and tested in the IC under two different temperature regimes: standard (room) temperature of 23°C and low temperature of 4°C. All the data acquired from IC were normalized with respect to the mass of cementitious materials in the mixture.

As shown in Figures 7(a) and 7(b), the addition of nano-TiO₂ to both, the room temperature cured and the low temperature cured OPC pastes, increases the values of the heat flow, as indicated by the higher maximum heights of the peaks for specimens with nano-TiO₂ (dotted lines) compared to the heights of the peaks for pastes without nano-TiO₂ (solid lines). Furthermore, the main hydration peak for pastes with nano-TiO₂ appears earlier (i.e., it is shifted to the left) when compared to the main hydration peaks for pastes without nano-TiO₂ (as indicated by the black arrows shown in Figure 7). That observations agree well with the TGA results reported in Section 3.1.

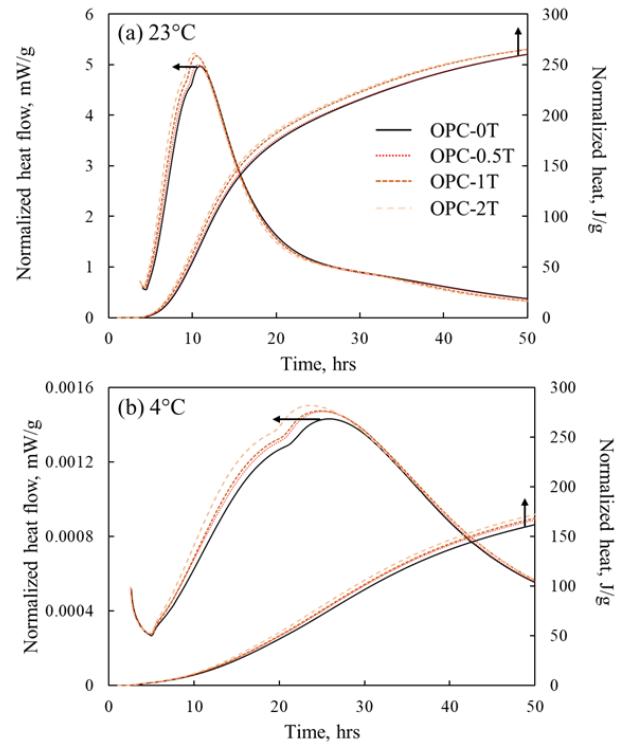


Figure 7. The normalized heat flow and normalized cumulative heat curves for OPC pastes cured at: (a) room temperature and (b) low temperature.

As shown in Figure 7(b), when the curing temperature was low, the hydration reactions slowed down significantly, as both heat flow and cumulative heat peaks were much lower than the results shown in Figure 7(a). The 50 h reaction period was just long enough to capture the majority of the heat flow peak for OPC pastes. Again, the addition of nano-TiO₂ seems to be more effective in accelerating the

hydration process when curing temperature was low. The time shift of the main hydration peaks due to the addition of nano-TiO₂ was larger for pastes cured at low temperature, (see Table 5).

Table 5. The time shift of the max. value of the heat flow peak due to the addition of nano-TiO₂ to OPC pastes (in comparison to the peak of pastes without nano-TiO₂).

Curing Temperature	Mixture	Time shift of the max temperature peak, min.
23°C	OPC-0.5T	-14
	OPC-1T	-26
	OPC-2T	-43
	OPC-0.5T	-40
4°C	OPC-1T	-59
	OPC-2T	-129

The normalized heat flow and the normalized cumulative heat curves for fly ash pastes cured at room and low temperatures are presented in Figures 8(a) and 8(b), respectively. The trends with respect to the effects of nano-TiO₂ on the acceleration of hydration observed in fly ash pastes were the same as those observed in the OPC pastes (Figure 7).

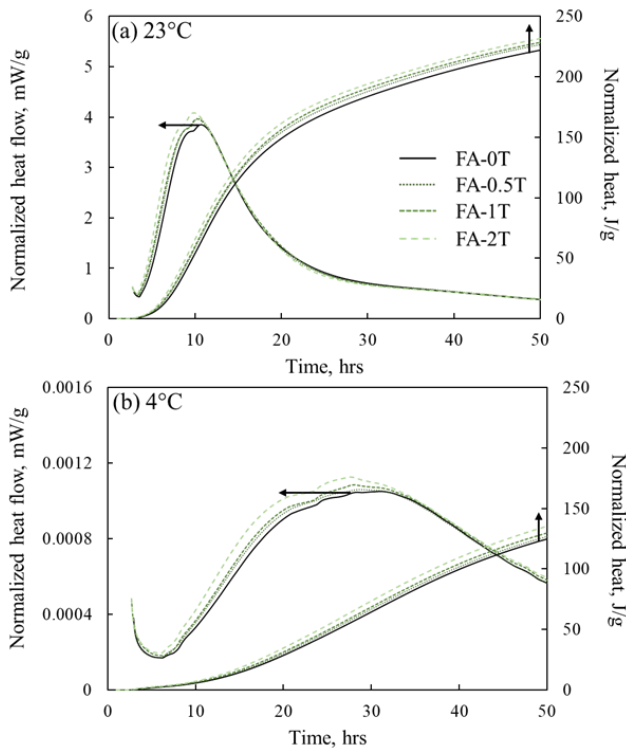


Figure 8. The normalized heat flow and the normalized cumulative heat curves for fly ash pastes cured at: (a) room temperature and (b) low temperature.

As shown in Table 6, the acceleration of the main hydration peak for low temperature cured fly ash pastes containing nano-TiO₂ was considerably higher

than that observed for the same type of pastes but cured at room temperature.

Table 6. The time shift of the max. value of the heat flow peak due to the addition of nano-TiO₂ to fly ash pastes (in comparison to the peak of pastes without nano-TiO₂).

Curing Temperature	Mixture	Time shift of the max temperature peak, min.
23°C	FA-0.5T	-20
	FA-1T	-26
	FA-2T	-50
	FA-0.5T	-143
4°C	FA-1T	-178
	FA-2T	-207

In summary, the test results obtained from the IC experiments corroborate the main conclusions derived from the TGA data, namely that nano-TiO₂ is more effective in accelerating the hydration in cases when curing temperature is low and when fly ash is used as a replacement for part of the cement.

3.3 Thermal indicator of the setting time of nano-TiO₂ modified pastes

As mentioned in Section 2.3.3, a thermal indicator of the setting time can be obtained from the IC data. For a given mixture, the thermal indicator of the setting time is a relative value, that can be correlated with a physical setting time determined using such methods as ASTM C191-21 [33]. This test methods can be used to determine the time of setting of hydraulic cement by means of the Vicat needle.

Figure 9 shows an example of how to obtain the thermal indicator of the setting time from the IC data.

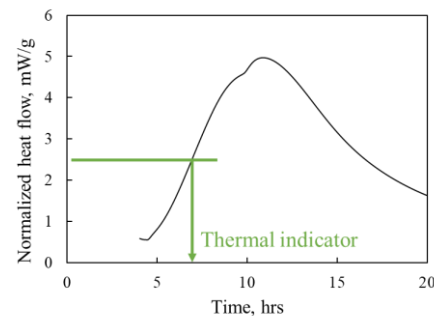


Figure 9. An example illustrating the way to obtain the thermal indicator of setting time using the heat flow curve from the IC experiment.

Shown in Figure 10 is the variation in the setting time (based on the thermal indicator data from the IC method) for both, the OPC and fly ash mixture as a function of the level of nano-TiO₂ addition and the curing temperatures. As can be seen, the addition of nano-TiO₂ shortens the setting time for both, the OPC and fly ash mixtures, regardless of the curing temperatures.

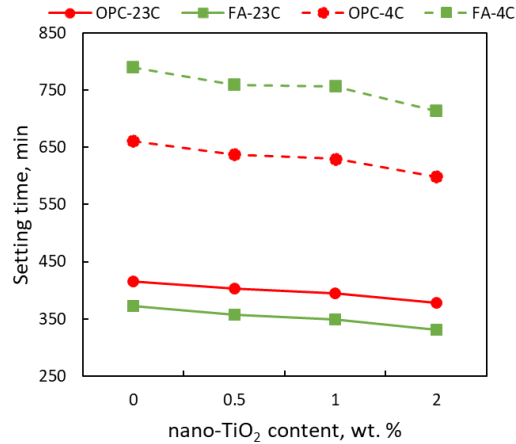


Figure 10. The variation in the setting time (based on the thermal indicator data from the IC method) as a function of the nano-TiO₂ addition for the OPC and fly ash pastes cured at room (23°C) and low (4°C) temperatures.

Table 7 shows an example of the actual values of the shortening of setting times for OPC and fly ash pastes containing 2% of nano-TiO₂ addition and cured at room and low temperatures.

Table 7. Shortening of the setting time (based on the thermal indicator data from the IC method) for OPC and fly ash pastes with 2% of nano-TiO₂ cured at room and low temperatures.

Curing Temperature	Mixture	Shortening of setting time, min [†]
23°C	OPC	38
	Fly ash	41
4°C	OPC	63
	Fly ash	76

[†] calculated with respect to setting time of specimens without nano-TiO₂ addition

When comparing the values of the shortening of the setting time, it can be observed that nano-TiO₂ seems to be more effective in accelerating the setting when the curing temperature is low compared to room temperature for both OPC and fly ash mixtures (~70 min. vs. ~40 min.). These observations agree with the results from the TGA tests presented in section 3.1, which indicated formation of higher amounts of the hydration products in the same type of cementitious systems.

3.4 The influence of the nano-TiO₂ on the compressive strength of OPC and fly ash mortars

The variation of the compressive strength of the OPC and fly ash mortars with and without the addition of nano-TiO₂ as a function of age and the curing temperature is shown in Figure 11. For mortars cured at room temperature, (Figure 11(a)), the addition of

0.5 wt.% of nano-TiO₂ improved the compressive strength of the OPC mortars cured for 3, 7, and 28 days. Somewhat smaller improvements were also observed for room temperature cured fly ash mortars, especially at 3 and 7 days.

Similarly, the improvement of compressive strength can also be observed for the case of low temperature curing (Figure 11(b)). As previously mentioned, the addition of nano-TiO₂ can lead to an accelerated hydration process, which can reduce the porosity within the paste matrix (also reported by [34]). Therefore, the bulk strength of mortars can be enhanced. A significant increase in compressive strength of fly ash mortars at 28 days can be observed when cured at a low temperature (as indicated by the black arrow in Figure 11(b)). This, again, is an indicator that nano-TiO₂ is more effective when the curing temperature is low.

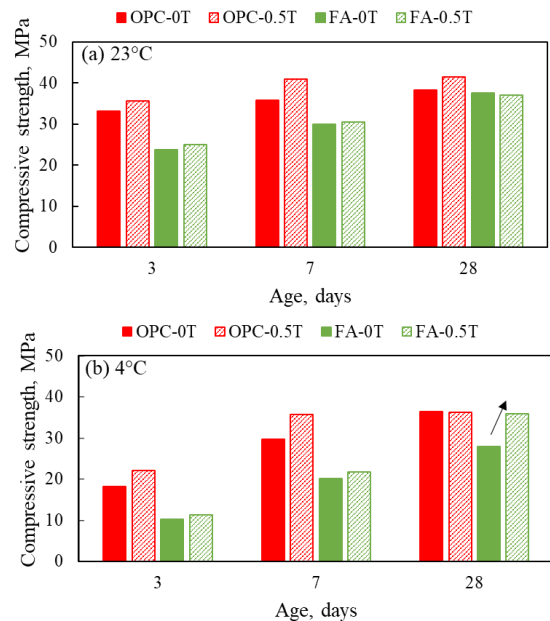


Figure 11. The variation of the compressive strength of OPC and fly ash mortars with age when cured at: (a) room (23°C) temperature and, (b) low (4°C) temperatures.

4. CONCLUSIONS

This paper focused on the study of the effects of addition of nano-TiO₂ on the hydration process and compressive strength development of the OPC and fly ash cementitious systems (pastes and mortars) cured at the standard (23°C) and low (4°C) temperatures. The results collected during the study support the following conclusions:

- As indicated by the IC data, the addition of nano-TiO₂ accelerated the hydration process of both, the OPC and fly ash pastes. The acceleration effects intensified with the increase in the addition level of the nano-TiO₂, and were more

pronounced in the cementitious systems cured for shorter periods of time, especially those cured at the low temperature. Specifically, the IC data suggest that the addition of nano-TiO₂ accelerates the appearance of the main hydration peaks in pastes, especially in fly ash pastes. For low curing temperature such acceleration can be 3-7 times (in terms of the length of the time shift) higher than that observed for room curing temperature.

- For fly ash pastes, the effect of the addition of nano-TiO₂ on the quantitative increases in the amount of hydration products (Q_{Iahp}) was higher at early ages (3 and 7 days) than at later ages (28 days), regardless of curing temperatures. At later ages, the addition of nano-TiO₂ seems to be more effective in accelerating hydration of specimens cured at low temperature.
- Thermal indicators of setting time, inferred from the IC results, show that the addition of nano-TiO₂ shortened the setting of OPC and fly ash mixtures, especially those cured at low temperature.
- The 0.5% addition of the nano-TiO₂ increased the compressive strength of both, the OPC and the fly ash mortars, when compared to reference samples (i.e., samples without the addition of nano-TiO₂).

ACKNOWLEDGEMENTS

This work was supported by the Joint Transportation Research Program administered by the Indiana Department of Transportation and Purdue University. The content of this paper reflect the views of the authors, who are responsible for the facts and the accuracy of the data presented herein, and does not necessarily reflect the official views or policies of the Federal Highway Administration and the Indiana Department of transportation, nor do the content constitutes a standard, specification, or regulation. The authors also gratefully acknowledge the help of Vito Francioso and Carlos Moro-Martinez in preparation of some of the test specimens.

REFERENCES

1. Lothenbach, B., Scrivener, K., Hooton, R.D., 2011. Supplementary cementitious materials. *Cem. Concr. Res.*, 41(12): 1244–1256.
2. Thomas, M., 2007. Optimizing the Use of Fly Ash in Concrete. Portland Cement Association, 24.
3. Jerath, S., Hanson, N., 2007. Effect of Fly Ash Content and Aggregate Gradation on the Durability of Concrete Pavements. *J. Mater. Civ. Eng.*, 19(5): 67–375.
4. Yu, J., Li, G., Leung, C.K.Y., 2018. Hydration and physical characteristics of ultrahigh-volume fly ash-cement systems with low water/binder ratio. *Constr. Build. Mater.*, 161: 509–518.
5. Kosmatka, S. H., Wilson, M. L., 2016. Design and Control Design and Control of Concrete Mixtures, 16th eddit.
6. Bilodeau, A., Sivasundaram, V., Painter, K.E., Malhotra, V.M., 1994. Durability of concrete incorporating high volumes of fly ash from sources in the U.S. *ACI Mater. J.*, 91(1): 3–12.
7. Berry, E.E., Malhotra, V.M., 1980. FLY ASH FOR USE IN CONCRETE - A CRITICAL REVIEW. *J. Am. Concr. Inst.*, 77,(2): 59–73.
8. Verian, K. P., Behnood, A., 2018. Effects of deicers on the performance of concrete pavements containing air-cooled blast furnace slag and supplementary cementitious materials. *Cem. Concr. Compos.*, 90: 27–41.
9. Xu, G., Shi, X., 2018. Characteristics and applications of fly ash as a sustainable construction material: A state-of-the-art review, *Resources, Conservation and Recycling*, 136: 95–109.
10. Wawrzęńczyk, J., Juszczak, T., Molendowska, A., 2016. Effect of Binder Composition on the Structure of Cement Paste and on Physical Properties and Freeze-Thaw Resistance of Concrete. in *Procedia Engineering*, 161: 73–78.
11. Valenza, J.J., Scherer, G.W., 2007. A review of salt scaling: I. Phenomenology. *Cement and Concrete Research*.
12. Molendowska, A., 2019. Scaling Resistance of Concretes Made with Fly Ash Cement. *IOP Conf. Ser. Mater. Sci. Eng.*, 471: 032024.
13. Mohseni, E., Miyandehi, B.M., Yang, J., Yazdi, M.A., 2015. Single and combined effects of nano-SiO₂, nano-Al₂O₃ and nano-TiO₂ on the mechanical, rheological and durability properties of self-compacting mortar containing fly ash. *Constr. Build. Mater.*, 84: 331–340.
14. Salemi, N., Behfarnia, K., 2013. Effect of nano-particles on durability of fiber-reinforced concrete pavement. *Constr. Build. Mater.*, 48: 934–941.
15. Li, Z., Ding, S., Yu, X., Han, B., Ou, J., Multifunctional cementitious composites modified with nano titanium dioxide: A review. *Compos. Part A Appl. Sci. Manuf.*, 111: 115–137.
16. Li, Z., 2017. Effect of nano-titanium dioxide on mechanical and electrical properties and microstructure of reactive powder concrete. *Mater. Res. Express*, 4(9): 095008.
17. Mohseni, E., Naseri, F., Amjadi, R., Khotbehsara, M.M., Ranjbar, M.M., 2016. Microstructure and durability properties of cement mortars containing nano-TiO₂ and rice husk ash. *Constr. Build. Mater.*, 114: 656–664.
18. ASTM C-150M-21, 2021. Standard Specification for Portland Cement Annu. B. *ASTM Stand.*, I: 1–8.

- 19.C. ASTM, 2010. Standard Specification for Coal Fly Ash and Raw or Calcined Natural Pozzolan for Use. Annu. B. ASTM Stand., 3–6.
- 20.ASTM C494/C494M–19, 2019. Standard Specification for Chemical Admixtures for Concrete. ASTM Int., 1–10.
- 21.I. Division of Construction Management, 2020. DIVISION 900 – MATERIALS DETAILS.
- 22.ASTM C305/C305-20, 2020. Standard Practice for Mechanical Mixing of Hydraulic Cement Pastes and Mortars of Plastic Consistency.
- 23.ASTM C 109/C 109M-21, 2021. Standard test method for compressive strength of hydraulic cement mortars. Annual Book of ASTM Standards, 04: 9.
- 24.Scrivener, K., Snellings, R., Lothenbach, B., 2016. A practical guide to microstructural analysis of cementitious materials.
- 25.Hager, I., 2013. Behaviour of cement concrete at high temperature. Bull. Polish Acad. Sci. Tech. Sci., 61(1):145–154.
- 26.Scrivener, K., Ouzia, A., Juilland, P., Kunhi Mohamed, A., 2019. Advances in understanding cement hydration mechanisms. Cem. Concr. Res., 124: 105823.
- 27.ASTM C1702-17, 2017. Standard test method for measurement of heat of hydration of hydraulic cementitious materials using isothermal conduction calorimetry. Annu. B. ASTM Stand., 1–9.
- 28.ASTM C1679, 2017. Standard Practice for Measuring Hydration Kinetics of Hydraulic Cementitious Mixtures Using Isothermal Calorimetry. Am. Soc. Test. Mater. West Conshohocken, PA, USA., 1–15.
- 29.Jalal, M., Fathi, M., Farzad, M., 2013. Effects of fly ash and TiO₂ nanoparticles on rheological, mechanical, microstructural and thermal properties of high strength self compacting concrete. Mech. Mater., 61: 11–27.
- 30.Nazari, A., Riahi, S., The effect of TiO₂ nanoparticles on water permeability and thermal and mechanical properties of high strength self-compacting concrete. Mater. Sci. Eng. A, 528(2): 756–763.
- 31.Zhang, M., Li, H., Pore structure and chloride permeability of concrete containing nano-particles for pavement. Constr. Build. Mater., 25(2): 608–616.
- 32.Moro, C., El Fil, H., Francioso, V., Velay-Lizancos, M., Influence of water-to-binder ratio on the optimum percentage of nano-TiO₂ addition in terms of compressive strength of mortars: A laboratory and virtual experimental study based on ANN model. Constr. Build. Mater., 120960.
- 33.ASTM C191-21, 2021. Standard Test Method for Time of Setting of Hydraulic Cement by Vicat Needle. Annu. B. ASTM Stand., 15(02).
- 34.Francioso, V., Moro, C., Martinez-Lage, I., Velay-Lizancos, M., 2019. Curing temperature: A key

factor that changes the effect of TiO₂ nanoparticles on mechanical properties, calcium hydroxide formation and pore structure of cement mortars. Cem. Concr. Compos., 104.